

Early accretion of chondrule dust rims. A. Carballido¹, C. Xiang¹, R.D. Hanna², L. S. Matthews¹, and T. W. Hyde¹.
¹Center for Astrophysics, Space Physics and Engineering Research (CASPER), One Bear Place #97283, Baylor University, Waco, TX, 76798-7283, USA. ²Jackson School of Geosciences, University of Texas, Austin, TX, 78712, USA.

Introduction: A critical step in the planetesimal formation process is the growth of solids from the sub-millimeter to meter scales. It has been suggested that this growth is enabled by the collisional aggregation of dust-coated chondrules [1,2], the igneous, spheroidal inclusions found in chondritic meteorites. The dust coatings, known as fine-grained rims (FGRs), are hypothesized to form from accretion of nebular dust onto chondrules [3,4]. FGRs may have enabled chondrules to stick together and form the building blocks of asteroids, and thus provide insight into the collisional history of chondrite parent bodies. However, the mechanical evolution of FGRs, and in particular the compacting processes that turned fluffy FGRs into low-porosity structures observed in the laboratory, remain poorly understood. The aim of our work is to fill that knowledge gap by investigating the early FGR accretion stage, as well as the more energetic aggregate- and parent-body-compaction stage.

In order to achieve our goal, we are performing numerical simulations of dust coagulation and of compaction of chondritic material. We are also determining the 3D morphology of FGRs from samples of minimally-altered CO, CR and CV chondrites. In this way, our laboratory measurements will provide a benchmark against which our simulations can be contrasted. Specifically, we are focusing on three FGR properties: porosity, thickness and grain alignment.

Methods: Numerical. 1) *Initial FGR structure.* We are using a discrete-element code developed at CASPER [5-7] to simulate accretion of both ellipsoidal and spherical micron-sized dust grains onto millimeter-sized chondrules. In particular, by using ellipsoidal grains we are able to determine the preferred alignment of dust grains within FGRs, in addition to FGR porosity and thickness (Fig. 1). 2) *Collision-induced FGR compaction.* In order to calculate the effect of parent-body collisions on FGR compaction within chondritic material, we are employing the iSALE2D shock physics code [8-10]. Chondrules are treated as zero-porosity forsterite disks embedded in a porous dunite matrix. A proof-of-concept simulation setup for unrimmed chondrules is shown in Fig. 2. The next step is to surround chondrules with porous dunite FGRs. This is work in progress.

Experimental. We are in the process of measuring FGRs within a suite of CV, CR, and CO chondrites that have experienced limited aqueous alteration and thermal metamorphism. Rim porosity will be calculated from electron probe microanalysis analytical totals. Rim thickness will be calculated from 3D measurements of

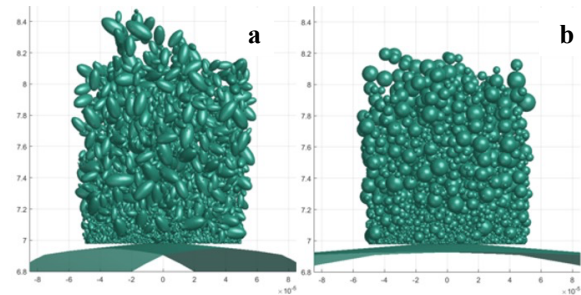


Figure 1: Rim growth on a 100- μm -radius patch on the surface of a 700- μm -radius chondrule using a) ellipsoidal and b) spherical monomers. Data from horizontal slices through the rims are used to calculate the porosity and grain alignment as a function of the distance from the chondrule surface.

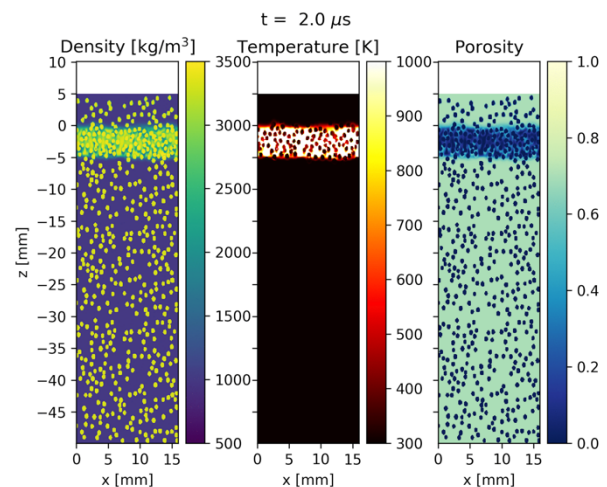


Figure 2: Snapshot of a shock wave traveling from top to bottom through a mixture of unrimmed chondrules embedded in a porous matrix. The shock is applied to the surface $z = 0$ mm at time $t = 0$ s.

FGRs in X-ray computed tomography (XCT). Grain alignment will be computed by a fabric strength parameter [11] calculated from electron backscatter diffraction.

Preliminary Results: Numerical. 1) *Initial FGR structure.* In Fig. 3 we show that rims comprised of ellipsoidal monomers (with a 3:1:1 aspect ratio) are more porous than rims comprised of spherical monomers with the same volume. The larger average cross-sectional area makes it more difficult for incoming elliptical monomers to pass through and fill in the pores. Final rim

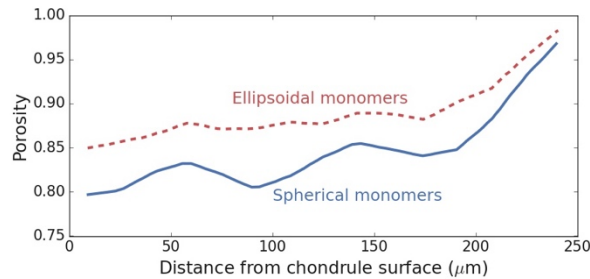


Figure 3: Radial profile of FGR porosity for rims made of ellipsoidal and spherical monomers.

porosities will be examined through simulation of rimmed-chondrule collisions and shocks.

2) Collision-induced FGR compaction. Figure 4 shows the behavior of bulk porosity of the chondritic mixture of Fig. 2 as a function of shock strength, which is parameterized by the impact speed between two parent bodies of the same dunite composition. The fractional area occupied by the (unrimmed) chondrules is 0.2. The three curves represent three different times after impact.

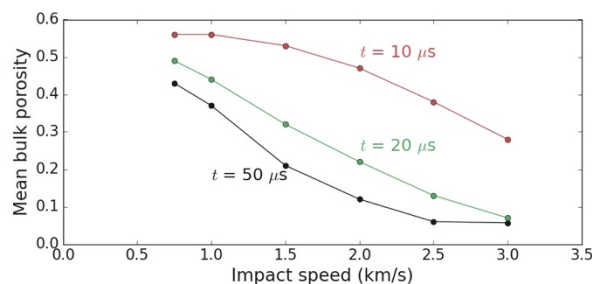


Figure 4: Mean bulk porosity of the chondritic mixture of Fig. 2 as a function of parent body impact speed, at three different times after impact.

As expected, the mixture becomes more compacted as the impact speed increases.

Experimental. We have scanned 2 COs (MIL 05024 and MIL 07193) and 2 CVs (RBT 04302 and RBT 04143) with XCT, all of which contain rimmed chondrules (Fig. 5). We are in the process of segment-ing out the chondrules and their rims for measurement of 3D FGR rim morphology and to check for evidence of impact compaction among the chondrules and rims [12,13].

Future Work: Additional numerical simulations of FGR accretion will be performed with the LIGGGHTS granular mechanics code [14], in order to capture the effect of FGR restructuring. Numerical studies of FGR accretion like these can be used to calibrate collisional experiments of FGR formation that use chondrule analogs, such as we are also designing (please see abstract titled “Experimental Study of Chondrule Rim Formation” by T. Hyde et al. in this Conference). For the purpose of

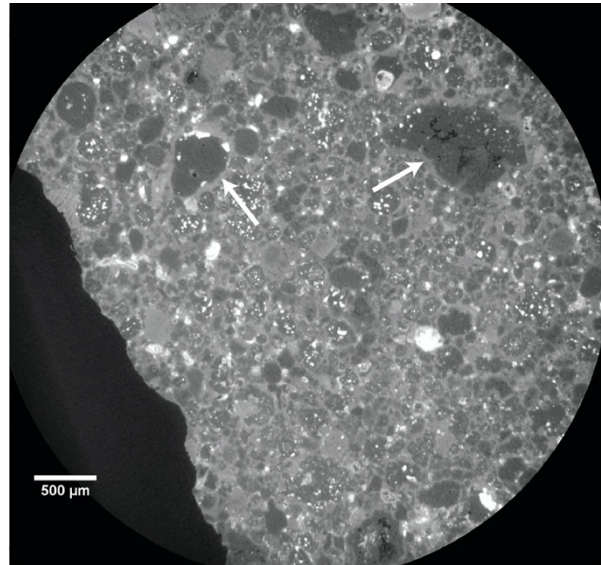


Figure 5: XCT scan of CO MIL 07193. White arrows indicate prominent fine-grained rims.

studying impact-induced FGR compaction, iSALE will be modified to allow the inclusion of rims surrounding chondrules, similarly to [15].

References: [1] Ormel, C. W. et al. (2008), *ApJ*, 679, 1588. [2] Simon, J. I. et al. (2018), *Earth Planet. Sci. Lett.*, 494, 69. [3] Metzler, K. et al. (1992) *Geochim. Et Cosmochim. Acta*, 56, 2873. [4] Cuzzi, J. N. (2004), *Icarus*, 168, 484. [5] Matthews, L. S. et al. (2007), *IEEE Transactions on Plasma Science*, 35(2), 260. [6] Xiang, C. et al. (2019), *Icarus*, 321, 99. [7] Xiang, C. et al (2021), *Icarus*, 354, id. 114053. [8] Amsden, A. A. et al. (1980) LANL Report, LA-8095:101p. [9] Collins, G. S. et al. (2004) *M&PS*, 39:217–231. [10] Wünnemann, K. et al. (2006) *Icarus*, 180:514–527. [11] Woodcock, N. H., and Naylor, M. A. (1983), *J. Struct. Geol.* 5, 539. [12] Hanna, R. D. & Ketcham, R. (2018), *Earth Planet. Sci. Lett.* 481, 201. [13] Hanna, R. D. et al. (2015) *Geochim. Cosmoch. Acta* 171, 256. [14] Kloss, C., et al. (2012) *Prog. Comput. Fluid Dyn.*, 12, 140. [15] Davison, T. M. et al. (2016), 79th Ann. Meeting of the Meteoritical Society, #6374.

Acknowledgements: Support for this work is provided by NSF grant 2008493. We gratefully acknowledge the developers of iSALE-2D, including G. Collins, K. Wünnemann, D. Elbeshausen, T. Davison, B. Ivanov and J. Melosh. U.S. Antarctic meteorite samples are recovered by the Antarctic Search for Meteorites (ANSMET) program which has been funded by NSF and NASA, and characterized and curated by the Department of Mineral Sciences of the Smithsonian Institution and Astromaterials Curation Office at NASA Johnson Space Center.